Supplementary Figure Legends

Supplementary Figure 1, related to Figure 1. Ablation of *Gclc* does not impair Treg cell expansion.

Naïve T cells were isolated from *Gclc*$^{fl/fl}$ and *Foxp3*^{cre}-*Gclc*$^{fl/fl}$ mice and induced to differentiate *in vitro* into Th0 cells by incubation with anti-(α)CD3 antibody plus αCD28 and IL2, or into iTregs by incubation with αCD3, αCD28, IL2, and TGFβ. **(A)** Intracellular staining and flow cytometric analysis of phosphorylated Stat5 (p-Stat5) in iTregs of the indicated genotypes. Data are the mean ± SEM (n=3) and representative of three independent trials. **(B)** Analysis of FSC and SSC of the iTregs in (A). Data are the mean ± SEM (n=3) and representative of five independent trials. **(C)** Intracellular staining and flow cytometric analysis of CD4^{+}Foxp3^{+} cells induced to differentiate into iTregs under suboptimal conditions. Data are the mean ± SEM (n=3) and representative of three independent trials. **(D)** RT-qPCR to measure *Gclc* mRNA expression in *Gclc*$^{fl/fl}$ and *Foxp3*^{cre}-*Gclc*$^{fl/fl}$ iTregs. Data are the mean ± SEM (n=3) and representative of three independent trials. **(E)** Mass-spectrometry based analysis of GSSG/GSH ratio in *Gclc*$^{fl/fl}$ and *Foxp3*^{cre}-*Gclc*$^{fl/fl}$ iTregs. Data are the mean ± SEM (n=3) and representative of two independent trials. **(F)** Flow cytometric analysis of ROS in *Gclc*$^{fl/fl}$ and *Foxp3*^{cre}-*Gclc*$^{fl/fl}$ iTregs as detected by DCF-DA staining. Data are the mean ± SEM (n=3) and representative of three independent trials. **(G)** Flow cytometric analysis of CD4^{+}Foxp3^{+} nTregs isolated from thymus of 4 week old *Gclc*$^{fl/fl}$ and *Foxp3*^{cre}-*Gclc*$^{fl/fl}$ mice. Data are the mean ± SEM (n=3) and representative of three independent trials. **(H)** Representative images of 8 week old *Gclc*$^{fl/fl}$ control and Foxp3^{cre}-*Gclc*$^{fl/fl}$ mice. **(I)** Histological analysis of H&E- stained sections of liver, lung and skin of 8 week old *Gclc*$^{fl/fl}$ and *Foxp3*^{cre}-*Gclc*$^{fl/fl}$ mice. Scale bars, 500 μm. Data are representative of three mice/group. **(J)** Sections of the skin and lung tissues from the mice in (G) were stained with αMac-3 to detect macrophages. Scale bars, 500 μm. Data are representative of three mice/group. *p < 0.05.

Supplementary Figure 2, related to Figure 2. *Foxp3*^{cre}-*Gclc*$^{fl/fl}$ mice develop spontaneous autoimmunity.

(A-B) Quantification of total naïve (CD44^{lo} CD62L^{hi}) and effector (CD44^{hi} CD62L^{lo}) subsets of CD4^{+} (left) and CD8^{+} (right) T cells isolated from (**A)** spleen and (**B)** lymph nodes (LN) of *Gclc*$^{fl/fl}$ control and *Foxp3*^{cre}-*Gclc*$^{fl/fl}$ mice. Data are the mean ± SEM (n=3) and representative

of three independent trials. **(C)** Splenic T cells from female *Foxp3*^{cre}-*Gclc*$^{fl/fl}$ and *Gclc*$^{fl/fl}$ mice were analyzed by flow cytometry to quantify effector and naïve T cells as in (A). Data are the mean ± SEM (n=3) and representative of three independent trials. **(D)** Flow cytometric analysis of Tbet expression of splenic CD4$^+$ T cells of *Gclc*$^{fl/fl}$ and *Foxp3*^{cre}-*Gclc*$^{fl/fl}$ mice. Data are the mean ± SEM (n=3) and representative of five independent trials. **(E-G)** T cells were isolated from the colonic lamina propria of *Gclc*$^{fl/fl}$ and *Foxp3*^{cre}-*Gclc*$^{fl/fl}$ mice and analyzed by flow cytometry to quantify (**E**) CD4$^+$ and CD8$^+$ T cells, (**F**) effector (CD44^{hi} CD62L^{lo}) CD4$^+$ and CD8$^+$ T cells, and (**G**) IFNγ-producing CD4$^+$ T cells. Data are the mean ± SEM (n=3) and representative of three independent trials. **(H-I)** Flow cytometric analysis of (**H)** CD4$^+$ CXCR5$^+$ PD1$^+$ follicular T helper cells and **(I)** CD19$^+$ B220$^+$ CD95$^+$ GL-7$^+$ GC B cells among splenocytes of 8 week old *Gclc*$^{fl/fl}$ and *Foxp3*^{cre}-*Gclc*$^{fl/fl}$ mice. Data are the mean ± SEM (n=3) and representative of five independent trials. **(J)** ELISA to detect IgG1, IgG2a, IgG3, and IgA in serum of 8 week old *Gclc*$^{fl/fl}$ and *Foxp3*^{cre}-*Gclc*$^{fl/fl}$ mice. Each symbol represents an individual mouse. Data are the mean ± SEM (n=11) and representative of two independent trials. *p < 0.05.

Supplementary Figure 3, related to Figure 3. An absence of *Gclc* does not affect Treg stability but does impair suppressive capacity.

(A) Flow cytometric determination of the expression of the indicated surface markers by *Gclc*$^{fl/fl}$ and *Foxp3*^{cre}-*Gclc*$^{fl/fl}$ iTregs. Data are representative of 4 trials. **(B)** Intracellular staining and flow cytometric analysis of Helios (top) and IRF4 (bottom) *Gclc*$^{fl/fl}$ and *Foxp3*^{cre}-*Gclc*$^{fl/fl}$ iTregs. Data are the mean ± SEM (n=3) and representative of three independent trials. **(C)** *In vitro* suppression assay of iTregs that were incubated with control Tconv at the indicated ratios for 48 hr. Tconv proliferation was determined by ^{3}H-thymidine incorporation. Data are the mean ± SEM (n=3) and representative of three independent trials. **(D)** *In vitro* assay of suppressive activity of *Gclc*$^{fl/fl}$ and *Foxp3*^{cre}-*Gclc*$^{fl/fl}$ iTregs incubated at the indicated ratios with Tconv labeled with Cell-Trace Violet (CTV). Suppression was determined by flow cytometry as a decrease in Tconv proliferation. Data are representative of five independent trials. **(E)** RT-qPCR measurement of IL-10 mRNA levels in *Gclc*$^{fl/fl}$ and *Foxp3*^{cre}-*Gclc*$^{fl/fl}$ iTregs (left). Intracellular staining and flow cytometric determination of TGF-β production by *Gclc*$^{fl/fl}$ and *Foxp3*^{cre}-*Gclc*$^{fl/fl}$ iTregs (right). Data are the mean ± SEM (n=3) and representative of three independent trials. *p < 0.05.

Supplementary Figure 4, related to Figure 4. mTOR blockade restores immune homeostasis and Treg function in *Gclc*-deficient mice.

(A) Principal component (PC) analysis of RNA-seq data of iTregs of the indicated genotypes. **(B)** Volcano plot comparing mRNA levels of the indicated Treg-associated genes in *Foxp3*^{cre}-*Gclc*$^{fl/fl}$ *and Gclc*$^{fl/fl}$ iTregs. Downregulated (blue) and upregulated (red) transcripts are shown. **(C)** Flow cytometric analysis of p-mTOR and pS6 in splenic T cells isolated from YFP^{+} and YFP^{-} female *Gclc*$^{fl/fl}$ and *Foxp3*^{cre}-*Gclc*$^{fl/fl}$ mice. Data are the mean ± SEM (n=3) and representative of two independent trials. **(D)** Intracellular staining and flow cytometric analysis of pS6 and Foxp3 in *Gclc*$^{fl/fl}$ and *Foxp3*$^{eGPF\text{-}cre\text{-}ERT2}$-*Gclc*$^{fl/fl}$ iTregs incubated with 4-OHT. Data are the mean ± SEM (n=3) and representative of three independent trials. **(E)** *In vitro* assay of suppressive activity of *Gclc*$^{fl/fl}$ and *Foxp3*$^{eGPF\text{-}cre\text{-}ERT2}$-*Gclc*$^{fl/fl}$ iTregs that were incubated with 4-OHT prior to incubation with CTV-labeled Tconv at the indicated ratios. Data are representative of three independent trials. **(F)** *In vitro* assay of suppressive activity of *Gclc*$^{fl/fl}$ and Foxp3^{cre}-*Gclc*$^{fl/fl}$ iTregs that were transduced with retrovirus expressing empty vector (EV) or Stat5 and incubated with CTV-labeled Tconv at the indicated ratios. Data are representative of two independent trials. *p<0.05. **(G-L)** *Gclc*$^{fl/fl}$ and *Foxp3*^{cre}-*Gclc*$^{fl/fl}$ mice (8 weeks old) were i.p.-injected with vehicle or rapamycin every other day for 30 days, followed by sacrifice on day 30. Splenic T cells were isolated and subjected to flow cytometric analysis to identify **(G)** naïve (CD44^{lo} CD62L^{hi}) and effector (CD44^{hi} CD62L^{lo}) subsets of CD4^{+} (top) and CD8^{+} (bottom) T cells, **(H)** CD4^{+} CXCR5^{+} PD-1^{+} Tfh cells, **(I)** CD19^{+} B220^{+} CD95^{+} GL-7^{+} GC B cells, **(J)** Tbet expression, and **(K)** IFNγ expression. **(L)** Histological analysis of lung tissues that were resected from one *Gclc*$^{fl/fl}$ and one *Foxp3*^{cre}-*Gclc*$^{fl/fl}$ male mouse and stained with H&E (top) or αCD3 to detect T cells (bottom). Scale bars, 500 μm. Results are representative of 4 mice per group and two independent trials. **(M)** *In vitro* suppression assay of iTregs derived from *Gclc*$^{fl/fl}$ and Foxp3^{cre}-*Gclc*$^{fl/fl}$ mice, incubated with or without rapamycin prior to co-incubation with control Tconv labeled with Cell-Trace Violet (CTV) at the indicated ratios. Data are representative of three independent trials. **(N)** Flow cytometric determination of transduction efficiency as determined by CD90.1 expression by the retrovirally transduced *Gclc*$^{fl/fl}$ and *Foxp3*^{cre}-*Gclc*$^{fl/fl}$ iTregs. **(O)** *In vitro* suppression assay of iTregs of *Gclc*$^{fl/fl}$ and Foxp3^{cre}-*Gclc*$^{fl/fl}$ mice that were transduced with retrovirus expressing EV or Foxp3 and incubated with CTV-labeled Tconv at the indicated ratios. Data are

representative of three independent trials. For (G-K), data are the mean ± SEM (n=3) and representative of two independent trials. *p < 0.05.

Supplementary Figure 5, related to Figure 4. GSH modulates one-carbon metabolism and Nrf2 signaling.

(A) Barcode enrichment plot of the KEGG pathway GO:0006520 (Cellular amino acid metabolic processes) for *Gclc*$^{fl/fl}$ and *Foxp3*^{cre}-*Gclc*$^{fl/fl}$ nTregs. **(B)** Barcode enrichment plot of the KEGG pathway GO:0006730 (One-carbon metabolic process) of *Gclc*$^{fl/fl}$ and *Foxp3*^{cre}-*Gclc*$^{fl/fl}$ nTregs. **(C)** Intracellular staining and flow cytometric analysis of pS6 (left) and Foxp3 (right) in *Gclc*$^{fl/fl}$ and *Foxp3*^{cre}-*Gclc*$^{fl/fl}$ iTregs that were induced in normal or glycine-deficient medium. Data are the mean ± SEM (n=3) and representative of three independent trials. **(D)** Intracellular staining and flow cytometric analysis of Foxp3 in *Gclc*$^{fl/fl}$ and *Foxp3*^{cre}-*Gclc*$^{fl/fl}$ iTregs that were cultured in serine-deficient medium for the indicated times. Data are the mean ± SEM (n=3) and representative of three independent trials. **(E)** RT-qPCR to measure *ASCT2* mRNA expression in *Gclc*$^{fl/fl}$ and *Foxp3*^{cre}-*Gclc*$^{fl/fl}$ iTregs. Data are the mean ± SEM (n=7) and representative of two independent trials. **(F)** Barcode enrichment plot of the KEGG pathway GO:0072593 (reactive oxygen species metabolic process) of *Gclc*$^{fl/fl}$ and *Foxp3*^{cre}-*Gclc*$^{fl/fl}$ iTregs (top) and nTregs (bottom). **(G)** Heatmap showing normalized differential gene expression levels of NRF2 target genes in *Gclc*$^{fl/fl}$ and *Foxp3*^{cre}-*Gclc*$^{fl/fl}$ iTregs (left) and nTregs (right). **(H)** Intracellular staining and flow cytometric analysis to detect Foxp3 in *Gclc*$^{fl/fl}$ and *Foxp3*^{cre}-*Gclc*$^{fl/fl}$ iTregs cultured in normal medium, or treated with 100μM NAC or 0.5mM GSH. Data are the mean ± SEM (n=3) and representative of three independent trials. **(I)** Quantification of serine in *Gclc*$^{fl/fl}$ and *Foxp3cre-Gclc*$^{fl/fl}$ iTregs cultured in normal medium with/without 50μM L-phenylglycine. Data are the mean ± SEM (n=3) and representative of three independent trials. **(J)** *Asct1* mRNA expression (left) and intracellular staining and flow cytometric analysis of FoxP3 (right) of *Gclc*$^{fl/fl}$ vs *Foxp3*^{cre}-*Gclc*$^{fl/fl}$ iTregs that were nucelofected with ASCT1-specific sgRNAs or controls Data are the mean ± SEM (n=3) and representative of two independent trials. **(K)** Quantitation of formate secretion by *Gclc*$^{fl/fl}$ and *Foxp3*^{cre}-*Gclc*$^{fl/fl}$ iTregs that were left untreated or treated with 10μM SHMT inhibitor. Data are the mean ± SEM (n=3) and representative of two independent trials. **(L)** Intracellular staining and flow cytometric analysis to detect Foxp3 in *Gclc*$^{fl/fl}$ and *Foxp3*^{cre}-*Gclc*$^{fl/fl}$ iTregs that were left untreated or treated with 10μM SHIN2. Data are the mean ± SEM (n=3) and representative of three independent trials. **(M)** Determination by ^{3}H-

thymidine incorporation of the proliferation of iTregs treated as in (H). Data are the mean ± SEM (n=3) and representative of three independent trials. *p < 0.05.

Supplementary Figure 6, related to Figure 6. Glutathione controls glycolysis and the TCA cycle in Tregs.

(A) Flow cytometric analysis and quantitation of Glut-1 protein in *Gclc*$^{fl/fl}$ and *Foxp3*^{cre}-*Gclc*$^{fl/fl}$ iTregs. Data are the mean ± SEM (n=3) and representative of four independent trials. **(B)** Left: Scheme depicting glycolysis and the TCA cycle. Right: Quantitation of relative mass isotopomer distribution of citrate following incubation of the cells in (A) with [U-$^{13}C_6$]-glucose for 24 hr. Data are the mean ± SEM (n=3) and representative of two independent trials. **(C)** Intracellular staining and flow cytometric analysis to detect c-MYC expression by *Gclc*$^{fl/fl}$ and *Foxp3*^{cre}-*Gclc*$^{fl/fl}$ iTregs. Data are the mean ± SEM (n=3) and representative of three independent trials. **(D)** Intracellular staining and flow cytometric analysis to detect Foxp3+ cells among WT T cells that were transduced with retrovirus expressing empty vector (EV) or Foxp3. Data are the mean ± SEM (n=3) and representative of three independent trials. *p < 0.05.

Supplementary Figure 7, related to Figure 7: GSH depletion in human Tregs interferes with FoxP3 expression and Treg functionality.

(A) Mass isotopomer distribution of M+3 serine (left) and M+2 glutathione (right) in WT murine iTregs that were cultured with or without serine and incubated with [U-$^{13}C_6$]-glucose for 24 hr. Data are the mean ± SEM (n=4). **(B-D)** Naïve human T cells were isolated from among PBMCs from healthy donors and induced to differentiate into iTregs in the presence or absence of BSO. **(B)** Luminescence based quantification of GSH. Data are the mean ± SEM (n=4). **(C, D)** Intracellular staining and flow cytometric analysis to detect **(C)** Foxp3 and **(D)** pS6 in human iTregs cultured with/without BSO. Data are the mean ± SEM (n=3-4) and representative of two independent trials. **(E, F)** Intracellular staining and flow cytometric analysis to detect **(E)** pS6 expression and **(F)** Foxp3 in human iTregs cultured with/without BSO and with/without serine, as indicated. Data are the mean ± SEM (n=3-4) and representative of two independent trials. **(G)** Intracellular staining and flow cytometric analysis to detect Foxp3 in human iTregs that were cultured with/without BSO, with/without L-phenylglycine, and with/without PHGDH inhibitor, as indicated. Data are the mean ± SEM (n=3-4) and representative of two independent trials. **(H)** *In vitro* assay of suppressive

activity of human iTregs that were induced with/without BSO and incubated at the indicated ratios with human Tconv labeled with Cell-Trace Violet (CTV). Suppression was determined by flow cytometry as decreased Tconv proliferation. Data are representative of two independent trials. **(I-K)** *Gclc*$^{fl/fl}$ and *Foxp3*^{cre}-*Gclc*$^{fl/fl}$ mice (8 weeks old) were transplanted subcutaneously with MC38 colon adenocarcinoma cells. **(I)** Mean tumor volumes were determined at the indicated times. **(J)** Quantification of tumor weights (left) and representative macroscopic images (right) of tumors from *Gclc*$^{fl/fl}$ and *Foxp3*^{cre}-*Gclc*$^{fl/fl}$ mice at time of sacrifice. **(K)** Quantification of the indicated subsets of TILs in tumors of *Gclc*$^{fl/fl}$ and *Foxp3*^{cre}-*Gclc*$^{fl/fl}$ mice treated as in I. Data are mean ± SEM (n=5). *p<0.05.

Supplementary Figure 1

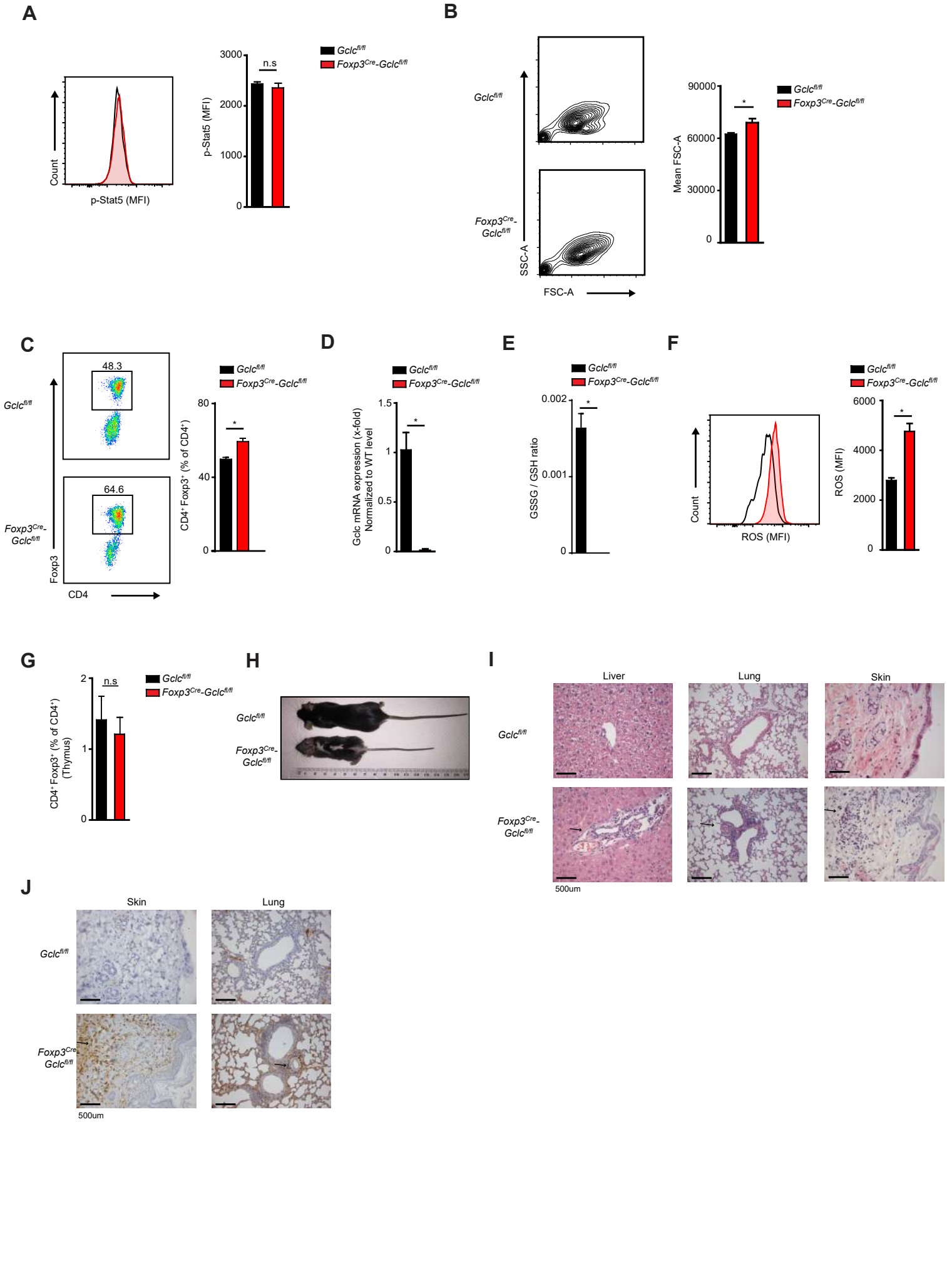

Supplementary Figure 2

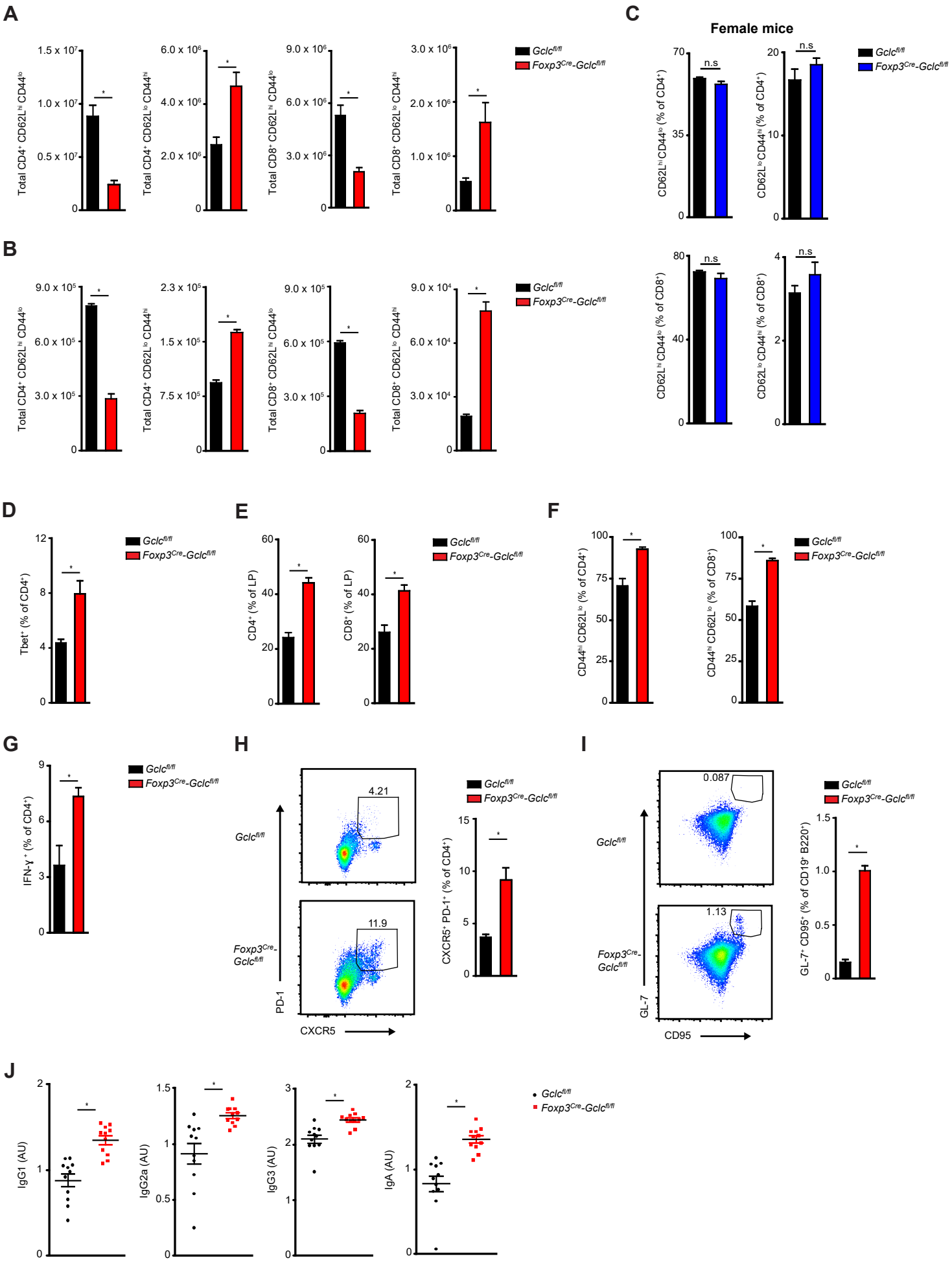

Supplementary Figure 3

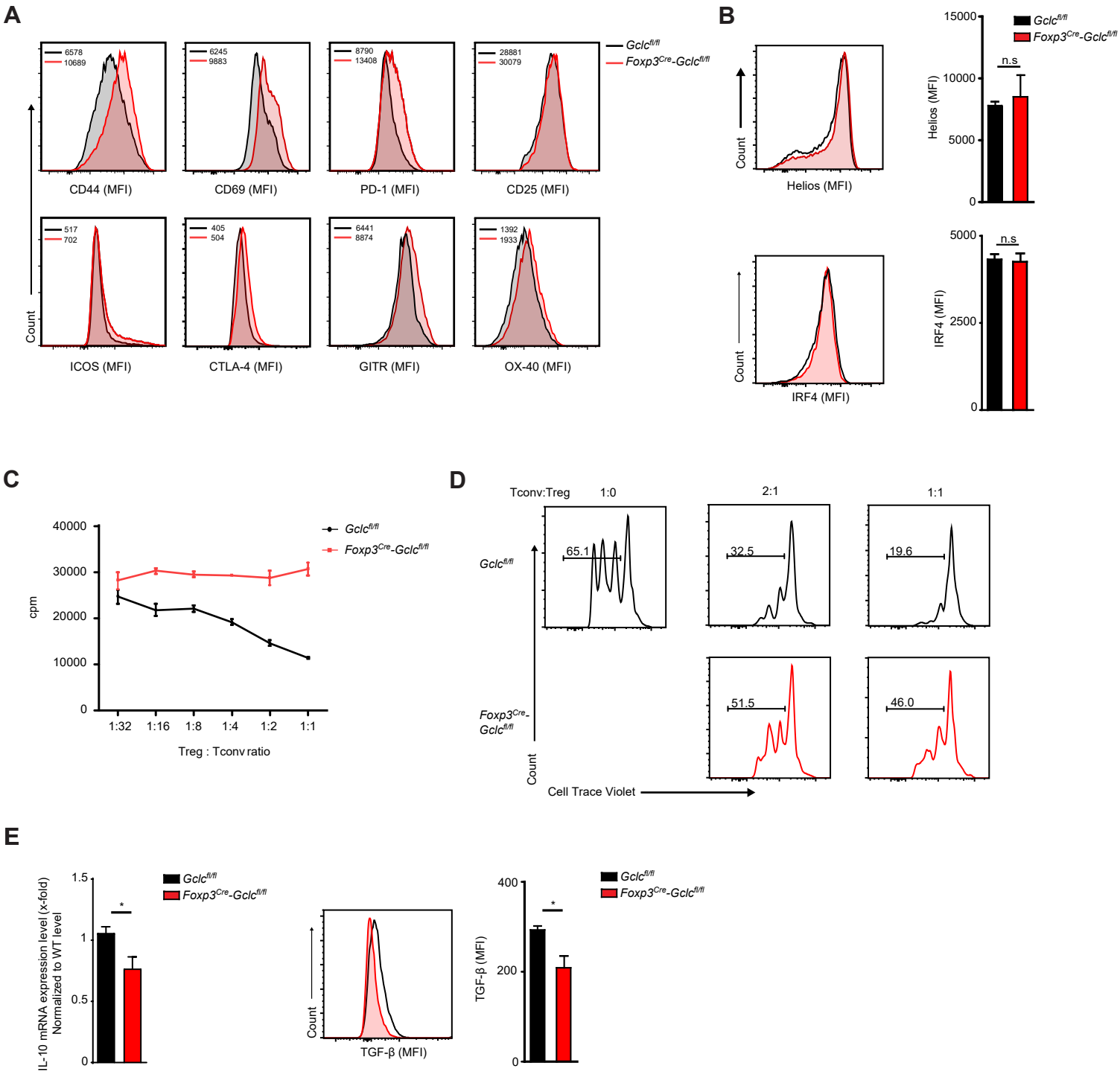

Supplementary Figure 4

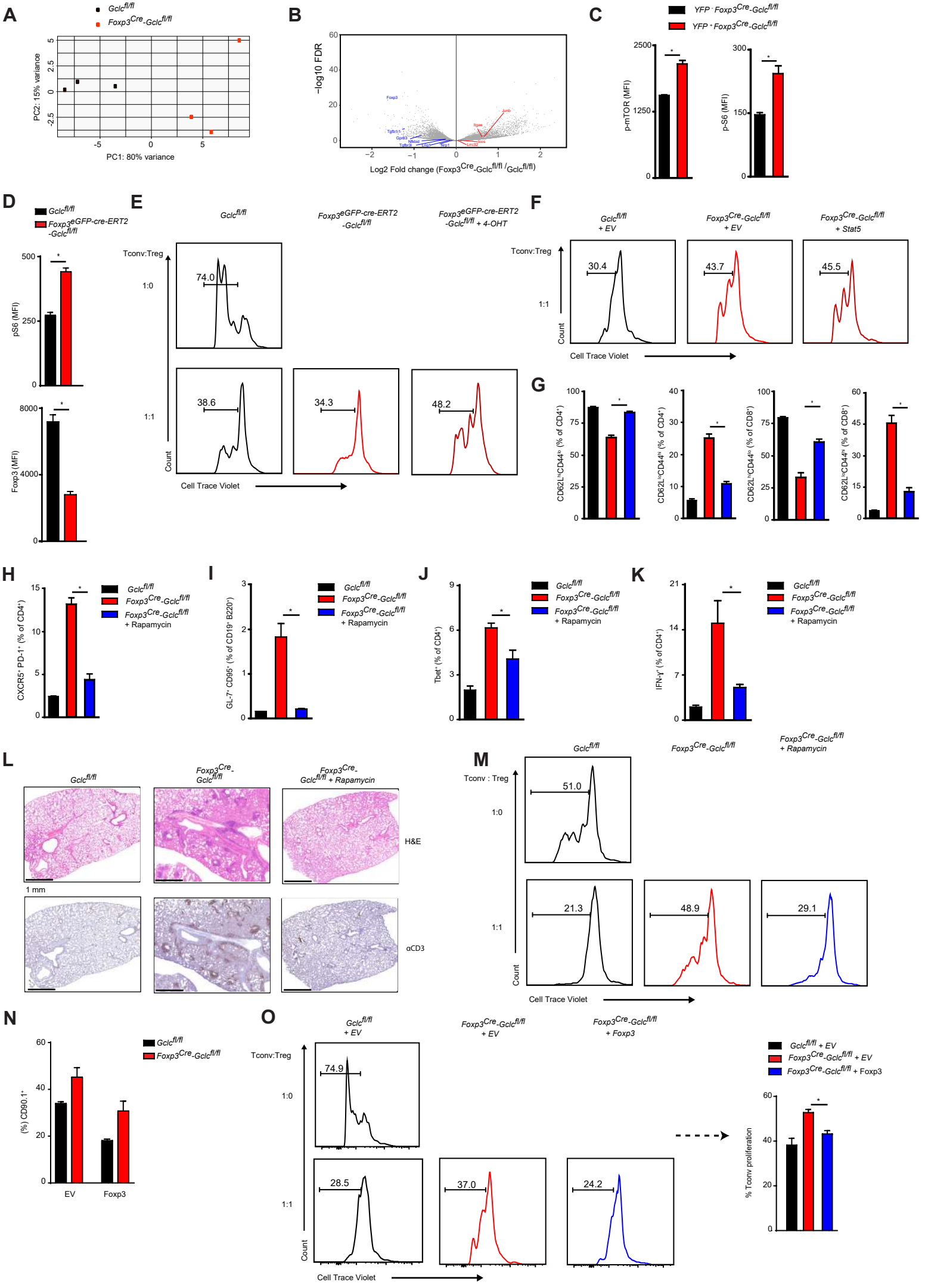

Supplementary Figure 5

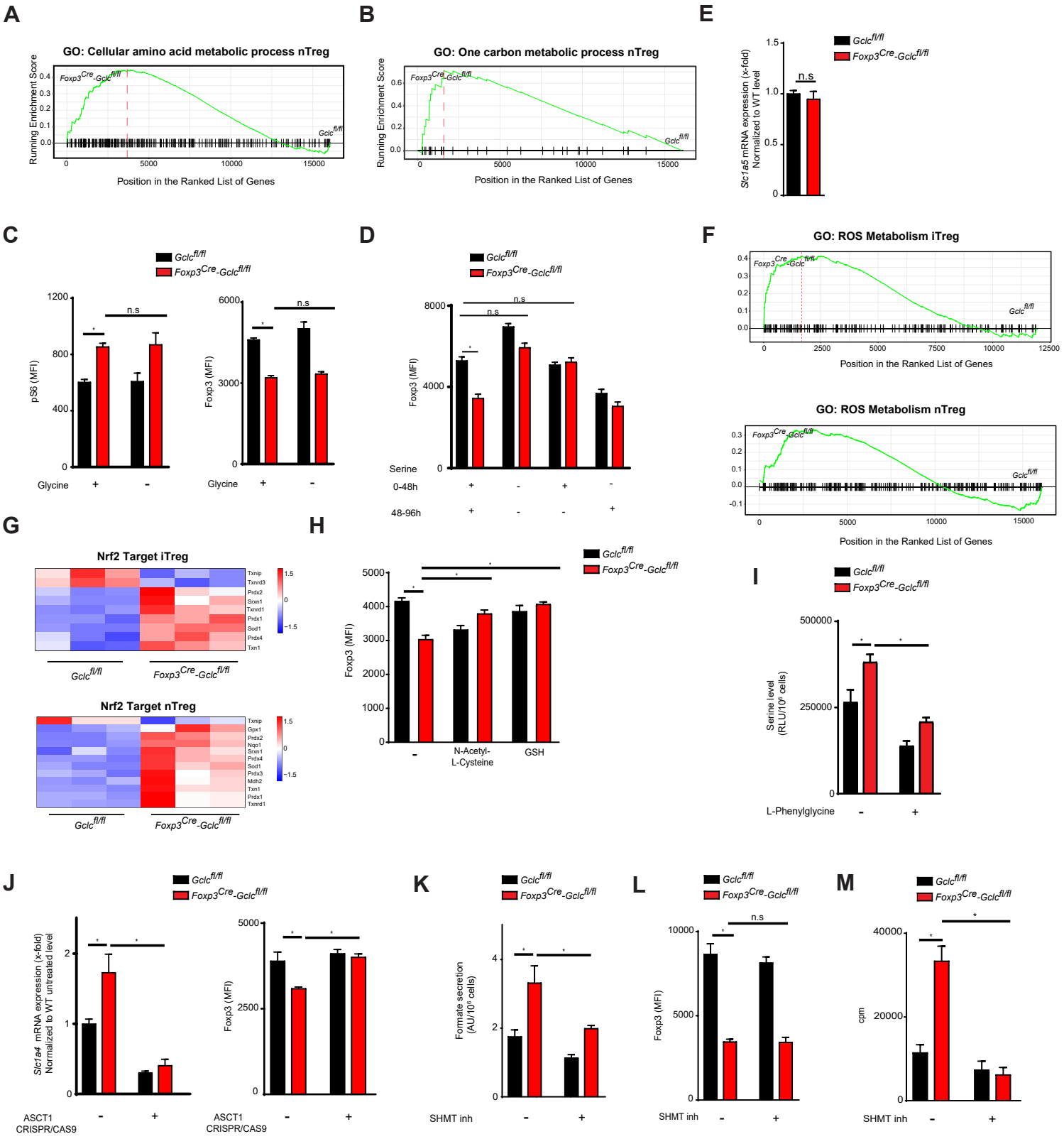

Supplementary Figure 6

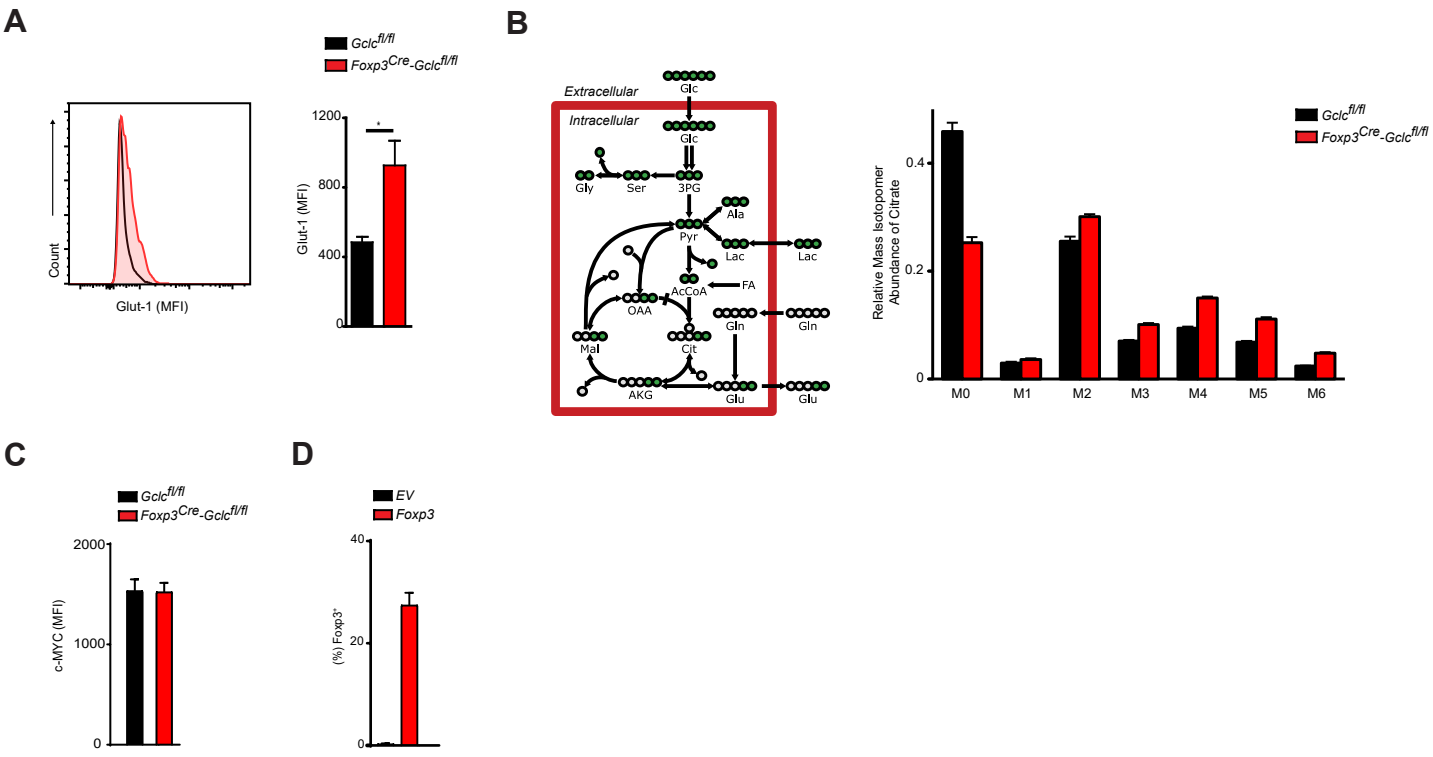

Supplementary Figure 7